Optimizing the Channel Selection and Classification Accuracy in EEG-Based BCI.
Mahnaz Arvaneh et al. (Chai Quek*)

IEEE Transactions on Biomedical Engineering (2011)

Presenter : SeungChan Lee

GIST, Dept. of Information and Communication, INFONET Lab.

Gwangju Institute of
Science and Technology

Background

- Channel selection problems in EEG-based BCI
  - A large number of EEG channels
    - It may include noisy and redundant signals. – degradation of performance
    - It needs a prolonged preparation time. – inconvenience in installation process
  - Selecting the least number of channels with required accuracy can balance both needs.
- Various channel selection methods
  - SVM based
    - Recursively eliminates the least-contributed channels based on classification accuracy.
  - Mutual information(MI) based
    - Rank the channels based on MI between channels and class labels
  - Common spatial filter(CSP) based
    - Directly select the channels according to their CSP coefficients
  - RCSP based
    - used sparse solutions of spatial filters

Background

- Research problems in EEG channel selection
  - How many channels are required for the best classification accuracy?
  - What is the minimum number of channels required to achieve the same accuracy as obtained by using all the channels?
- To address the research questions…
  - They proposed a sparse common spatial pattern(SCSP) algorithm.
  - The proposed algorithm minimizes the number of channels by sparsifying the common spatial filters within a constraint of classification accuracy.

CSP algorithm

- The CSP algorithm is effective in discriminating two classes of EEG data by maximizing the variance of one class while minimizing the variance of the other class.

- Summary of formula derivation
  - Let single trial EEG data $\mathbf{X} \in \mathbf{R}^{N \times S}$
    (N : the number of channels, S: the number of measurement samples)
  - The CSP algorithm projects **X** to spatially filtered **Z** as $\mathbf{Z} = \mathbf{WX}$
    (the rows of $\mathbf{W}$: the spatial filters, the columns of $\mathbf{W}^{-1}$: CSP)
  - Normalized covariance matrix $\mathbf{C} = \dfrac{\mathbf{XX}^{T}}{\mathrm{trace}(\mathbf{XX}^{T})}$

    trace(X) : sum of diagonal elements of **X**
  - $\mathbf{C}_{C} = \mathbf{C}_{1} + \mathbf{C}_{2} = \mathbf{F}_{C}\psi\mathbf{F}_{C}^{T}$
    $\mathbf{C}_{1}, \mathbf{C}_{2}$: Computed by averaging over multiple trials of EEG data
      $\mathbf{F}_{C}$: matrix of normalized eigenvectors
      ψ : diagonal matrix of eigenvalues
  - Whitening transformation matrix
  - Transformation of covariance matrices

CSP algorithm

- Summary of formula derivation
  - Whitening transformation matrix $\mathbf{P} = \sqrt{\psi^{-1}} \mathbf{F}_C^T$
  - Transformation of covariance matrices

  $$\mathbf{C}_1' = \mathbf{P}\mathbf{C}_1\mathbf{P}^T, \quad \mathbf{C}_2' = \mathbf{P}\mathbf{C}_2\mathbf{P}^T$$
  $$= \mathbf{U}\Lambda_1\mathbf{U}^T \qquad = \mathbf{U}\Lambda_2\mathbf{U}^T \qquad \Lambda_1 + \Lambda_2 = \mathbf{I}$$

  $\mathbf{C}_1', \mathbf{C}_2'$: share common eigenvectors,
  $\mathbf{U}$: eigenvectors matrix
  Λ : diagonal eigenvalues matrix
  - Apply CSP projection matrix $\mathbf{W} = \mathbf{U}^T\mathbf{P}$

  $$\mathbf{C}_1' = \mathbf{U}^T\mathbf{P}\mathbf{C}_1\mathbf{P}^T\mathbf{U} = \Lambda_1, \quad \mathbf{C}_2' = \mathbf{U}^T\mathbf{P}\mathbf{C}_2\mathbf{P}^T\mathbf{U} = \Lambda_2 \qquad \Lambda_1 + \Lambda_2 = \mathbf{I}$$

  - Because $\Lambda_1 + \Lambda_2 = \mathbf{I}$, the maximum variance of one class lead to the minimum variance of the another class.→ Optimal discrimination
  - Projection matrix **W** can be formulated as an optimization problem

  $$\min_{\mathbf{W}_i}\left(\sum_{i=1}^{i=m} \mathbf{w}_i\mathbf{C}_2\mathbf{w}_i^T + \sum_{i=m+1}^{i=2m} \mathbf{w}_i\mathbf{C}_1\mathbf{w}_i^T \right)$$

  $\mathbf{C}_i$: covariance matrix of class i

  $\mathbf{w} \in {}^{1 \times N}, i = \{1, \ , 2m\}$ indicate

  Subject to : $\mathbf{w}_i(\mathbf{C}_1 + \mathbf{C}_2)\mathbf{w}_j^T$

  $\mathbf{w}$ $(\mathbf{C} + \mathbf{C})\mathbf{w}^T$

$= 1,$

$= 1,$

CSP algorithm

$i = \quad i$

$\{1,$ first and last m rows
$2,$ of CSP projection $2m\}$
i, j matrix
$= \{1,$
$2, \qquad , 2m\}\ i \neq j$

SCSP algorithm

- Motivation
  - Sparsify the CSP spatial filters to emphasize on a limited number of channels with high variances between the classes
  - Discard the rest of the channels with low or irregular variances that may be due to noise or artifacts.
- Sparsity measurement
  - $l_1 / l_2 = \dfrac{\|\mathbf{x}\|_1}{\|\mathbf{x}\|_2}$

  - The sparsest possible vector(only a single element is nonzero) has a sparseness of one.
  - Non-sparsity measurement : l_1 / l_2 norm increases when the sparsity decreases.
- Modification of CSP algorithm

SCSP algorithm

- Modification of CSP algorithm
  - Include regularization parameter in optimization problem

$$\min_{\mathbf{w}_i}(1-r)\left(\sum_{i=1}^{i=m} \mathbf{w}_i \mathbf{C}_2 \mathbf{w}_i^T + \sum_{i=m+1}^{i=2m} \mathbf{w}_i \mathbf{C}_1 \mathbf{w}_i^T \right) + r \sum_{i=1}^{i=2m} \frac{\|\mathbf{w}_i\|_1}{\|\mathbf{w}_i\|_2}$$

$$\text{Subject to : } \mathbf{w}_i(\mathbf{C}_1 + \mathbf{C}_2)\mathbf{w}_i^T = 1, \ i = \{1,2, \ \ ,2m\}$$
$$\mathbf{w}_i(\mathbf{C}_1 + \mathbf{C}_2)\mathbf{w}_j^T = 1, \ i,j = \{1,2, \ \ ,2m\} \ i \neq j$$

  - Parameter $r(0 \leq r \leq 1)$ controls the number of removed channels and classification accuracy.
  - Non-linear optimization problem $\rightarrow$ solved using sequential quadratic programming(SQP) and augmented Lagrangian methods

SCSP algorithm

- Channel selection
    - From training set of two class motor imagery data, first two sparse spatial filters corresponding each class are obtained by solving the optimization problem.
    - Zero element channel → discard
      Non-zero element channel → select the channels
    - Importance order : apply ranking method(used maximum of the absolute values of the corresponding sparse spatial filter.

Datasets and processing

- Datasets
    - With a moderate number of channels (22 channels)
        - Dataset 2a from BCI competition 4
        - 9 subjects
        - Used only right and left hand motor imagery tasks
        - 72 trials training set + 72 trials testing set on each subjects
    - With a large number of channels (118 channels)
        - Dataset 4a from BCI competition 3
        - 5 subjects
        - Right hand and foot motor imagery tasks
        - 140 trials training set + 140 trials testing set on each subjects
- Data processing
    - Extract 0.5 ~ 2.5 seconds data samples after the visual cue
    - Apply 8 ~ 35Hz band-pass filter
    - (Training set) select optimal channels using first and last sparse spatial filter
    - (Test set) CSP retraining over selected channels and dataset spatially filtered using the first and last 3 spatial filters.
    - Variance of spatially filtered signal applied SVM classifier

Results and Discussion

- Performance comparison of l_1 and l_1 / l_2 Regularization term
    - Varying r value(different number of channels)
    - l_1 / l_2 norm based SCSP algorithm leads better classification accuracies when two different regularization based SCSP algorithm select same number of channels.
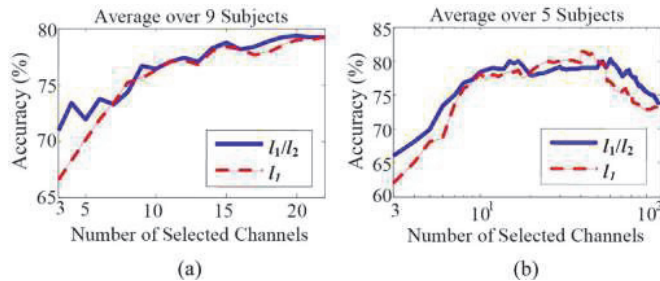
Results and Discussion

- Channel selection with different criteria
    - Two channel selection criteria
        - First criterion : maximizes the accuracy by removing noisy and irrelevant channels.(SCSP1)
        - Second criterion : minimizes the number of selected channels while maintaining the classification accuracy.(SCSP2)
    - Procedure
        - r was chosen from 0.01 to 0.99.
        - For each r, a set of selected channels was determined.
        - Using 10x10 fold cross validation on training set, compute classification accuracy with each set of the selected channels.
        - Optimal r was selected based on the accuracy.

Results and Discussion

● Channel selection with different criteria

(a)   (b)

(c)   (d)
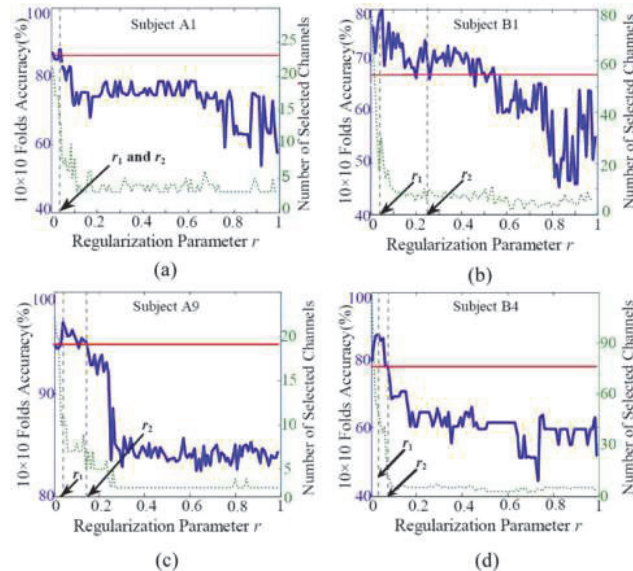
– Summary
   • the use of small values of r improved the accuracy by removing some noisy and redundant EEG channels, while increased values of r reduced the number of channels but also decreased the classification accuracy.
   • further increase of the r value did not yield further reduction in the number of selected channels.

Results and Discussion

– Classification accuracy vs. number of selected channels.
– About bellow table (overall 22 channel subjects)
   • Decreasing the number of channels is very effective without accuracy degradation.(SCSP1: reduced 40% of the channels, SCSP2: reduced 61.2% of the channels)
   • the proposed SCSP algorithm using both criteria yielded significantly better classification accuracies (average 9.45% more) compared to the use of three typical channels.

| | | | SCSP1 | | SCSP2 | |
Subject	All Ch Acc(%)	(C3,C4,Cz) Acc(%)	Acc (%)	♯ Selected Ch	Acc (%)	♯ Selected Ch
A1	90.97	75.69	91.66	13	91.66	13
A2	56.25	53.47	67.36	9	60.41	4
A3	96.52	93.05	97.91	14	97.14	12
A4	72.91	68.05	72.22	14	70.83	11
A5	63.88	53.47	65.27	11	63.19	9
A6	63.88	61.11	66.67	14	61.11	10
A7	79.86	57.63	84.72	19	78.47	15
A8	97.22	86.80	97.22	15	95.13	5
A9	91.66	88.88	91.66	10	93.75	5
Mean	79.23	70.90	81.63	13.22	79.07	8.55
Std	15.63	15.72	13.7	2.99	15.61	3.90
p-value	0.006	–	0.003	–	0.004	–

Dataset IIa, BCI Competition IV

P-value denotes the paired T-test between results of (C3,C4,CZ) and other results.
(CH: Channels, ACC: Accuracy, ♯ : Number).

Results and Discussion

- Classification accuracy vs. number of selected channels.
- About bellow table (overall 118 channel subjects)
  - Decreasing the number of channels is very effective without accuracy degradation.(SCSP1: reduced 81% of the channels, SCSP2: reduced 93% of the channels)
  - The results also show an average improvement of 11.5% in the classification accuracy compared to the use of three typical channels.

			SCSP1		SCSP2	
Subject	All Ch Acc(%)	(C3,C4,Cz) Acc(%)	Acc (%)	♯ Selected Ch	Acc (%)	♯ Selected Ch
B1	74.28	54.28	80.71	17	71.42	7
B2	94.28	80	97.14	12	95.71	10
B3	49.28	55	57.14	33	57.14	3
B4	77.14	70	85	36	77.85	10
B5	72.85	87.14	91.42	15	94.28	10
Mean	73.56	69.28	82.28	22.6	79.28	7.6
Std	16.06	14.69	15.38	11.05	16.19	3.08
p-value	0.535	–	0.043	–	0.023	–

Dataset IVa, BCI Competition III

P-value denotes the paired T-test between results of (C3,C4,CZ) and other results.
(CH: Channels, ACC: Accuracy, ♯ : Number).

Results and Discussion

- Spatial filter coefficient distribution
  - CSP filters have large weights in several unexpected locations.→ degradation of classification accuracies.
  - the SCSP filters have strong weights over the motor cortex areas and smooth weights over the other areas. → the proposed SCSP yielded filters that are neurophysiologically more relevant and interpretable.
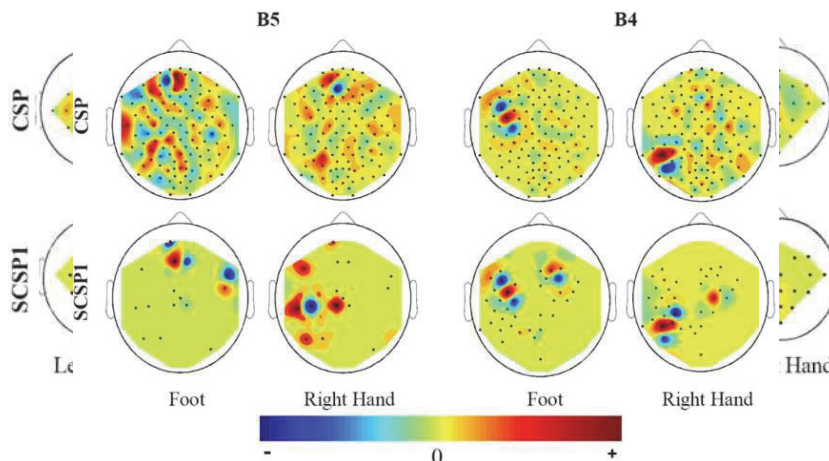
Conclusion

- They investigated the reduction of channels whereby the classification accuracy is constrained to an acceptable range.
- Two criterions
  - Using the first criterion yielded the best classification.
  - Using the second criterion retained the least number of channels.
- The proposed SCSP algorithm yielded an average improvement of 10% in classification accuracy compared to the use of typical three channels
- A visualization of the obtained sparse spatial filters
  - The proposed algorithm improved the results by emphasizing on a limited number of channels with high variances between the classes.

Compressed sensing in photoacoustic tomography

Lihong V. Wang.

Journal of Biomedical Optics 2010

Presenter Pavel Ni

Gwangju Institute of
Science and Technology

1

Contents

2

Introduction

- Photoacoustic formation sound waves, following light absorption in a material sample.
- For Photoacoustic effect the light intensity must vary periodically or as a single flash.
- The Photoacoustic effect is quantified by measuring the formed sound.
- By processing acquired signal map of absorbed light can be reconstructed.
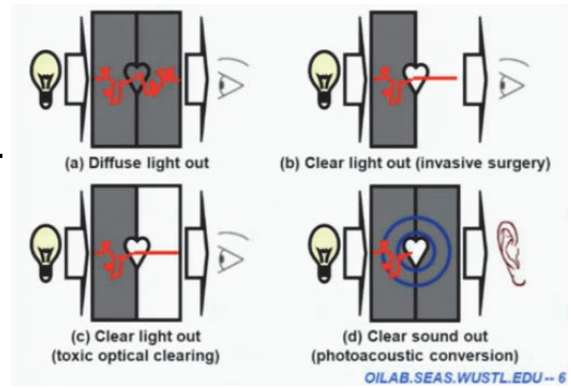
Pic. 1. Optical modalities compared to photoacoustic

- Tissues are irradiated by a pulsed laser
- Absorbed energy converted into heat
- Which further converted to thermoelastic expansion
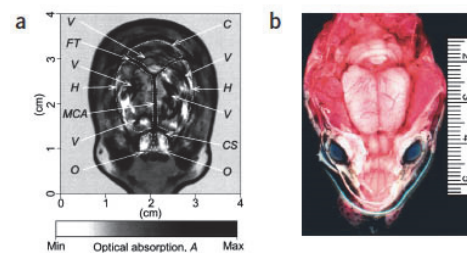- Initial pressure raise then propagates as ultrasonic waves

- Laser could be replaced by microwave or RF sources

Introduction
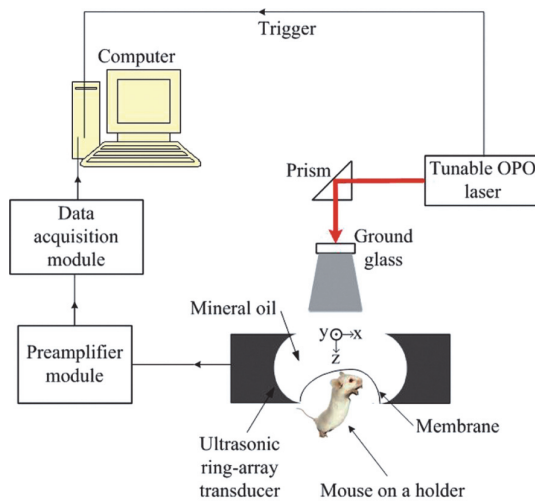
Pic. 2. Photoacoustic setup

Pic. 3. a) Noninvasive PAT image of the superficial layer of a rat brain acquired with the skin and skull intact
b) Open-skull photograph of the rat brain surface after PAT

- Unfocused ultrasonic transducer with 512 elements is placed outside of object
- 64-channel data acquisition module (DAQ) is used

Compressive sensing

Pressure measurement at detecting aperture $p(\vec{r},t)$

Initial pressure raises distribution $p_0(\vec{r})$

$$p(\vec{r},t) = \frac{d}{dx}\left[\frac{1}{4\pi c^3 t}\int d\vec{r}\,' p_0(\vec{r})\partial\left(t - \frac{|\vec{r}-\vec{r}\,'|}{c}\right)\right] \tag{1}$$

Forward problem which predicts $p(\vec{r},t)$ by $p_0(\vec{r})$
Where c-is a speed of sound, $\vec{r}$ is a position of ultrasonic sensor
Velocity potential $\varphi(\vec{r},t)$

$$p_0(\vec{r}) = \int_{s_0}\left[2p(\vec{r}_0,\bar{t}) - \frac{2\bar{t}\,\partial p(\vec{r}_0,\bar{t})}{\partial\bar{t}}\right]_{t=|r-r_0|} d\Omega_0 / \Omega_0 \tag{2}$$

Inverse problem which reconstruct $p_0(\vec{r})$ with $p(\vec{r},t)$
Where $\bar{t}=ct$, S_0 is the detecting aperture, $d\Omega_0/\Omega_0$ solid-angle weighting factor

Compressive sensing

x to represent $p_0(\vec{r})$ where each element of x is the average value of initial pressure per unit volume
Size of x depends on the field of view ($N_x*N_y*N_z$)

Vector y is velocity potential measured by all sensors as a function of time
Size of y is the number of detecting positions (L) times the number of temporal position (M)

Forward problem can be described as $y = \Phi x$
Where Φ is projection matrix

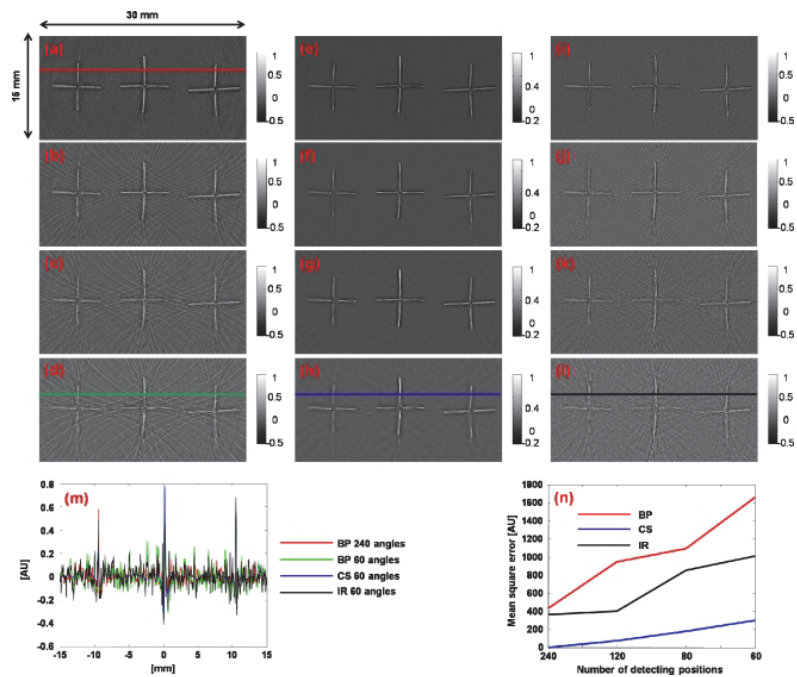Inverse problem can be written as $\bar{x} = \Phi^{-1}y$
Where $\bar{x}$ is reconstructed image

Φ containing $N_x*N_y*N_z*L*M$
Even for 256x256 image with measurement fro 512 positions, each position has 1024 time points   contain 3.4×10^{10} points (~256 GB)

Results

Pic. 4. (a) to (d) Images reconstructed using the BP method with 240, 120, 80, and 60 tomographic angles. (e) to (h) Images reconstructed using the CS method with 240, 120, 80, and 60 tomographic angles. (i) to (l) Images reconstructed using the traditional iterative reconstruction method with 240, 120, 80, and 60 tomographic angles. (m) Lines extracted from (a), (d), (h), and (l). (n) Comparison of the mean square errors of the three reconstruction methods.

Conclusion

They demonstrated the CS method using tissue-mimicking phantom with 3 human hair crosses with interval 10 mm. Laser pulses 10 Hz. 20 measurements at 240 different angles. Acquisition time was 8 min. Experiment shows that CS method can efficiently reduce the undersampling artifacts.
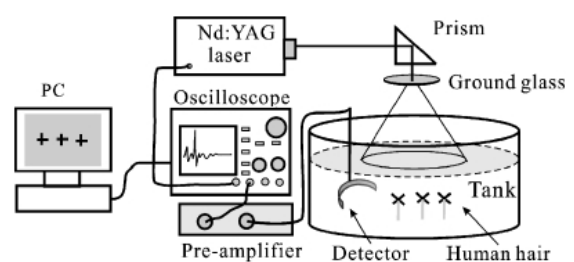
Pic. 5. used PA setup

Thank you

Toward Brain–Actuated Humanoid Robots: Asynchronous Direct Control Using an EEG–Based BCI

Yongwook Chae, Jaeseung Jeong, Sungho Jo

IEEE Transactions on Robotics.(2012.10)

Presenter : Soogil Woo

GIST, Dept. of Information and Communication, INFONET Lab.

Gwangju Institute of
Science and Technology

Introduction

- In the past, there have been numerous attempts to design and build full-bodied humanoid robots.

- The realization of a robotic system that understands human intentions and produces complex behaviors is needed, for disabled or elderly persons.

- The EEG-based BCI system for robots has been suggested in robotics and neural engineering fields because some elderly or disabled people can control robots naturally and intuitively by thinking while using this system.

- The active BCI can control an application using consciously intended brain signals without external events.

- BCI methods using sensorimotor rhythms belong to the active BCI.

- These methods classify specific motor images in a general sense through the power over the frequency ranges [e.g., mu (8–12 Hz) or beta (18–22 Hz)].

Introduction

- In a synchronous BCI system, sequential cues are provided at a fixed rate.

- Because a user cannot control the timing of motion commands, it tends to lower the information transfer rate (ITR).

- One main goal of EEG-based BCIs for human robot interaction is being able to command a robot directly by thinking.

- This paper describes a new brain-actuated humanoid robot navigation system that allows for asynchronous direct control of humanoid motions using the active BCI system.

- Their system provides five low-level motion commands (e.g., "stop," "turn the head to the left," "turn the head to the right," "turn the body," or "walk forward") by combining the classification of three motor imagery (MI) states (e.g., "left hand," "right hand," or "foot") with a posture-dependent control paradigm.

- To evaluate the proposed system, a humanoid robot navigation experiment in a maze was conducted with human subjects.

Methods

- Their proposed system has four key features.

- First, low-level commands make the humanoid turn at any angle and walk to any position.

- Second, five complex humanoid motions are controlled by three intentional mental states.

- Third, the subject can command the humanoid using asynchronous protocol.

- Fourth, their system does not employ a reactive but rather an active system.

Methods(System Description)

- The system consists of three main subsystems: the BCI system, the interface system, and the humanoid control systems.

- The BCI system classifies four user mental states.

- The non-control state is referred to as "rest" and the three MI states are referred to as "left hand", "right hand", and "foot".
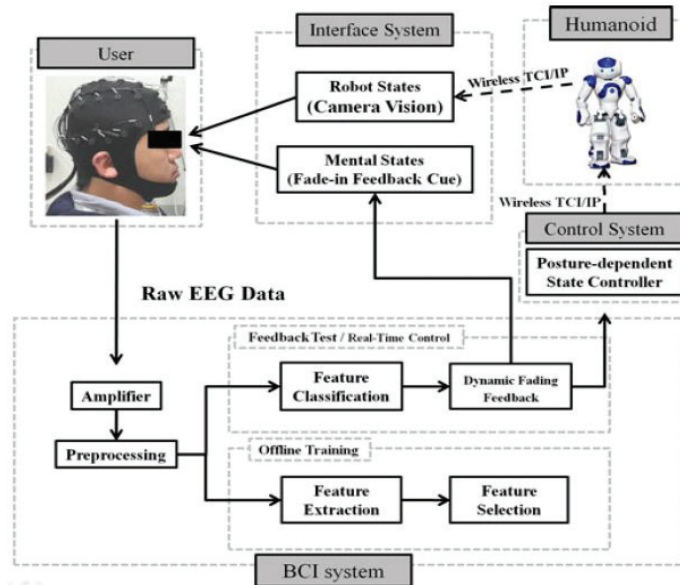
Methods(Experimental Protocol)

- 1) Offline training session

- 2) Selection of informative feature components and training of two classifiers

- 3) Online testing sessions

- 4) Checking the accuracy of the online session

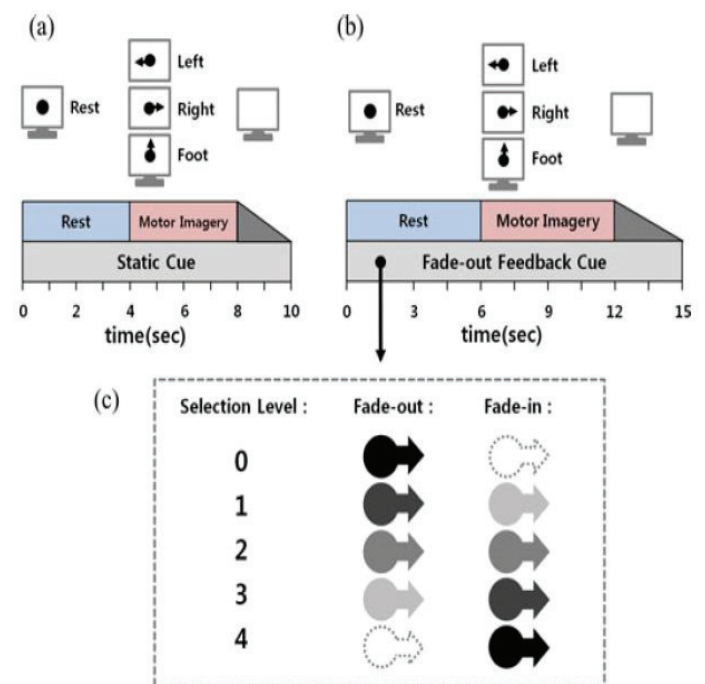- 5) Real-time humanoid navigation control experiment

Fig. 2.   (a) Offline training protocol: After the rest sessions, the subject is asked to imagine a motor imagery indicated by a static cue. (b) Online feedback testing protocol: 6 s are allowed to test the performance of the classification with dynamic fade-out feedback. (c) Dynamic fading feedback is used to secure a robust classification of a mental state from the ongoing EEG (see Section II-H).

Methods(Experimental Protocol)

- To verify the navigation performance of system, an indoor maze was designed.

- It was aimed to reduce the bias through an order of experiments (manual control or BCI control).

- If they missed any waypoints, they could skip them.

- Each subject conducted the experiment 3 times using the BCI system and one time through keyboard control for comparison.

(a)　　　　(b)
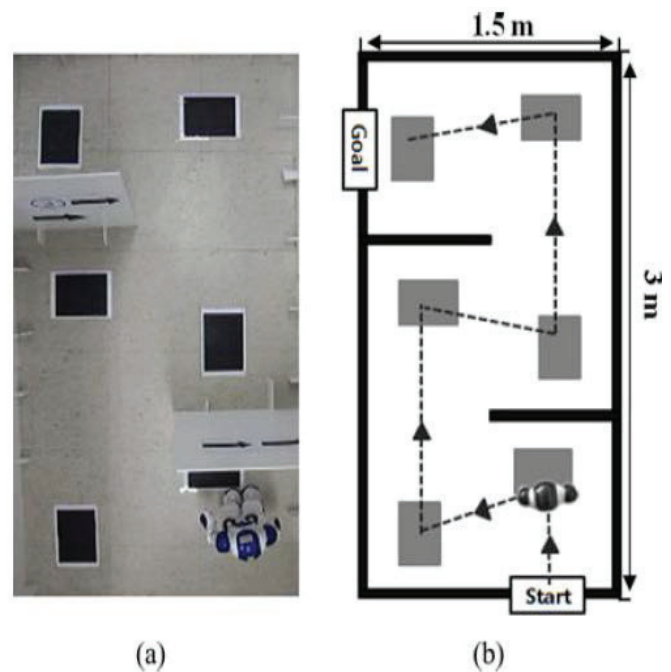
Methods(Data acquisition & Feature Extraction)

- In this paper, they applied this signal processing protocol to filter and detect the sensorimotor rhythm.

- An electrode at the vertex of the head was used as a reference, and extra electrode was used as a ground.

- The impedances of all of the electrodes were lower than 5 kΩ.

- For the real-time process, a total of 21 electrodes around the sensorimotor cortex were used to apply the large Laplacian filter over the nine frontocentroparietal locations based on the international 10-20 system as show in fig.
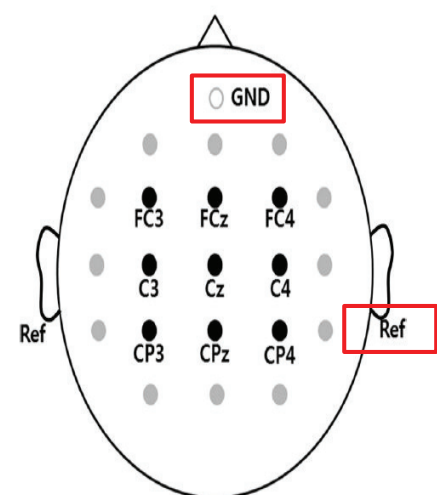

Fig. 4.　EEG electrode positions with respect to the international 10–20 system. Electrode positions marked with gray circles were only used to compute the spatial filter. The nine black circles indicate the electrode positions used as the main feature channels. All electrodes are referenced to the left and right mastoids.

Methods(Data acquisition & Feature Extraction)

- To extract amplitude features, every 250ms observation segment recorded for 2 s (500 samples) from nine channels was analyzed by the autoregressive algorithm, and the square root of power in 1Hz wide frequency bands within 4-36 Hz was calculated.

- In the offline training session, 32 feature vectors with 288 dimensions (9 channels * 32 frequency components) were collected within the MI and rest periods (4 s for each) for one trial.

- These feature vectors were used to select informative feature components and train the classifiers.

- During the online testing and real-time control session, the feature vectors were sampled from the selected informative feature components and these were used to produce real-time feedback and classification for the motion commands.

Methods(Feature Selection)

- In this study, the Fisher ratio was used to select informative feature components of each subject that can be interpreted as suitable channel–frequency bands.

- For the amplitude feature vector from the "rest" and MI states, let μ_{rest} and σ_{rest} denote the mean and variance, respectively, of the amplitude feature set from the "rest" state, and let μ_{MI} and σ_{MI} denote the mean and variance, respectively, of the amplitude feature set from the MI state.

- The Fisher ratio is defined as the ratio of the between-class variance to the within-class variance as follows:

$$fr = \frac{\sigma_{between}^2}{\sigma_{within}^2} = \frac{\left(\mu_{rest} - \mu_{MI}\right)^2}{\sigma_{rest}^2 + \sigma_{MI}^2}$$

- The Fisher ratio is a measure of the (linear) discrimination of two variables, and it can also be considered as a signal-to-noise ratio.
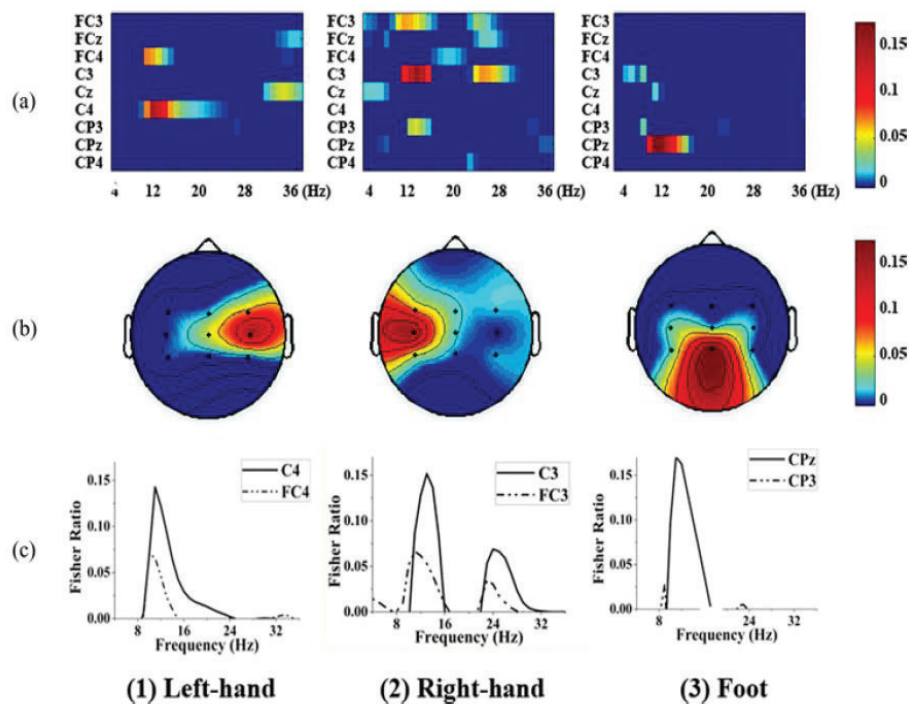
Methods(Feature Selection)

Fig. 5. Channel–frequency selection using the Fisher ratios from three sets of "rest" versus MI tasks. (a) Channel–frequency distribution of the Fisher ratios of subject A. (b) Topographical distribution of the Fisher ratios of subject A at the highest frequency bands (12, 14, and 10 Hz, respectively). The first two top-scoring channels for the "left-hand" imagery tasks were channels C4 and FC4, while channels C3 and FC3 were selected for the "right-hand" imagery tasks, and channels CPz and Cz were selected for the "foot" imagery tasks. (c) Spectral distribution of the Fisher ratios for subject A. For the "left-hand" imagery tasks, the maximum Fisher ratio of C4 was 0.15 at 12 Hz, and a 5-Hz window centered at 12 Hz was selected as the optimal frequency region.

Methods(Classification)

- To translate the intended EEG data into appropriate movement commands for the humanoid robot, the intentional activity classifier (IAC) and movement direction classifier (MDC) were employed.

- If the signals are interpreted as the MI state by the IAC, then the MDC classifies the specific MI state as either a "left hand", "right hand", or "foot" states.

- For the initial training, the features from the training trials between 0 and 4 s (e.g., rest period) were assigned to the "rest" class, and the signal segments between 4 and 8 s (e.g., MI period) were assigned to the MI class.

- For the training, the negative output values of the IAC denote the "rest" classes, while the positive output values of the IAC denote the MI classes.
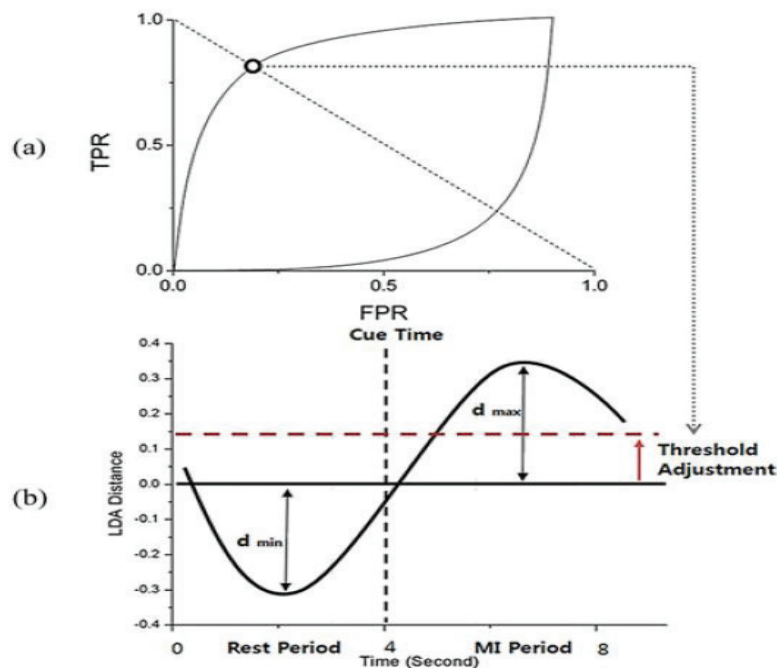
Methods(Classification)

Fig. 6. Time period selection using the LDA distance metric and determination of a classifier threshold. (a) ROC curve determines an appropriate threshold value and (b) a typical intention level curve of a subject to discriminate the rest and MI time periods. As the informative time period, a 1-s interval centered at the maximum and minimum LDA distance points was selected.

Methods(Dynamic Fading Feedback rule)

- Because the classification results of the sensorimotor rhythm based active BCI could generate the misclassification results, some normalization methods would be used to enable a smooth transition between class-specific feedbacks.

- In this study, the dynamic fading feedback rule was designed to avoid abrupt false classifications, as shown in fig.
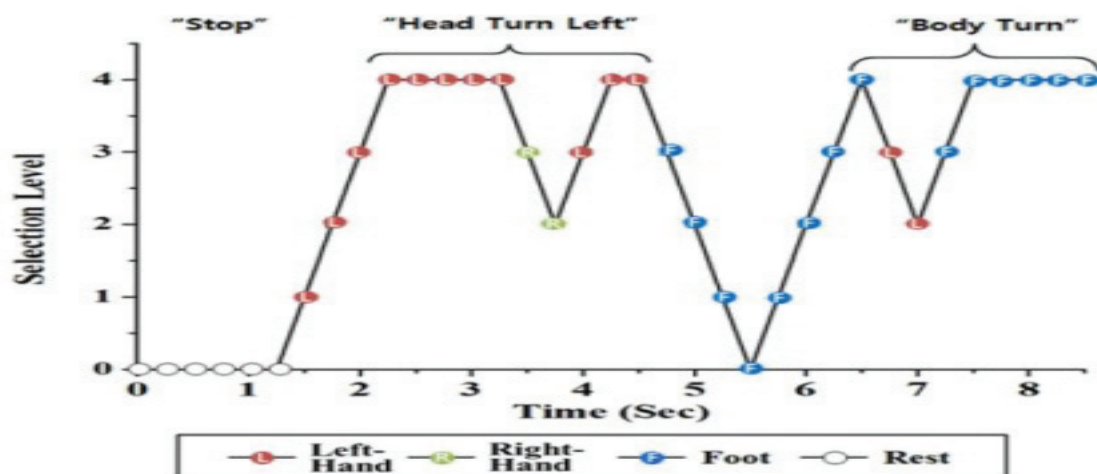

Fig. 8. Dynamic fading feedback rule. Variation of selection levels and classifications of a real-time BCI experiment over 8.5 s.

Methods(Dynamic Fading Feedback rule)

- 1) the candidate decision produced during the online feedback testing session and the real-time control session
- 2) the selection level associated with the confidence measurement of selected classifications.

➢ Rule 1: When the selection level is zero, the next first classification is newly set to be the candidate's decision.

➢ Rule 2: Whenever the classification result is identical to the candidate decision, the selection level is increased by 1; otherwise, the selection level is decreased by 1.

➢ Rule 3: When the selection level reaches 4, the control system confirms its decision and generates a motion command accordingly (i.e., "left," "right," or "forward").

➢ Rule 4: The fading feedback cues and the arrow and text shown on the display are transparentized according to the candidate's decision and its selection level.

Methods(Dynamic Fading Feedback rule)

- Fig. 8 illustrates an example of the command selection procedure.

- For the first 1 s, the consecutive "rest" commands appear.

- At 1.25 s, the four consecutive "left-hand" classifications increase the selection level up to 4, and then, the system generates a "left" command. The robot executes its motion accordingly through the control paradigm, as described in Fig. 7 (i.e., "head turn left").

- Next, consecutive "left-hand" classifications cause the robot to keep turning its head to the left up to 15∘ (3∘ per command).
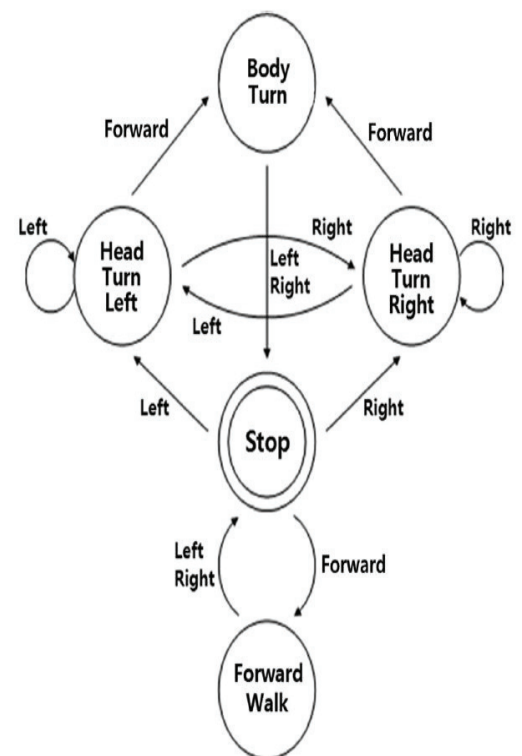

Fig. 7. Diagram of humanoid navigation control. (Left) Left-hand imagery. (Right) Right-hand imagery. (Forward) Foot imagery.

Methods(Evaluation)

- **1) Performance of the Brain–Computer Interface System**: (ITR)

$$I_d = \log_2 N + p \log_2 p + (1-p)\log_2\{(1-p)/(N-1)\}, \quad \text{ITR}=f_d \times I_d$$

- I_d is the bit rate (bits/trial) for the three mental state choices (N=3), p is the accuracy, and f_d is the decision rate (trial/min).

- **2) Navigation Performance**

✓ Total Time: total time taken to accomplish the task (in seconds);

✓ Traveled Distance: distance traveled to accomplish the task (in centimeters);

✓ Forward Steps: number of walking steps during forward movement;

✓ Turning Steps: number of walking steps to turn the robot body;

✓ Explored Angle: total turning angle of the robot head to explore the surrounding environment (in degrees);

✓ # Trans: number of transitions between the walking mode and the exploration mode;

✓ Waypoint: number of waypoints on which the robot

Results(Feature Selection)

- The Fisher ratios for the channel and frequency components and averaged discriminant values for the offline training period for each motor imagery and subject are illustrated.

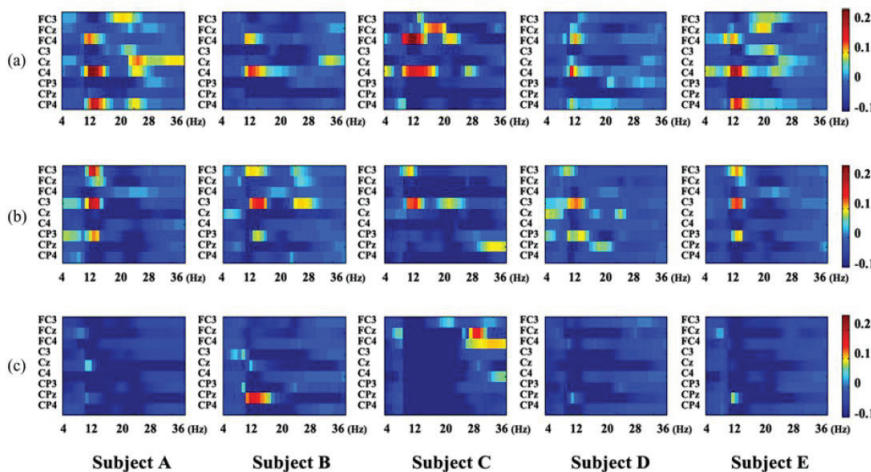- Table I describes the selected feature components of the five subjects.

Fig. 10. Channel–frequency distributions of Fisher ratios for all subjects for "left-hand," "right-hand," and "foot" imagery tasks. (a) Left. (b) Right. (c) Foot.

TABLE I
FEATURE SELECTION RESULTS

Subject	Left-hand		Right-hand		Foot	
	Ch	Freq	Ch	Freq	Ch	Freq
A	C4	9-13	FC3	10-14	Cz	8-12
	CP4	10-14	C3	9-13	CPz	7-11
B	C4	11-15	C3	12-16	CPz	10-14
	FC4	9-13	FC3	8-12	CP3	21-25
C	FC4	9-13	C3	9-13	FCz	26-30
	C4	10-14	FC3	7-11	FC4	28-32
D	C4	9-13	C3	10-13	CPz	8-12
	FC4	10-14	CP3	11-15	FC4	6-10
E	C4	9-13	C3	11-15	CPz	9-13
	CP4	10-14	FC3	11-15	FCz	6-10

Results(Navigation Performance)

- Tables II and III provide details about the performance of the two hierarchical classifiers (IAC and MDC) for the five subjects.

- Table II shows the number of offline training trials per mental task, the TPR and FPR of the IAC, and the accuracy of the MDC for each task.

- Table III shows the online testing performance achieved using the fading feedback rule for the given mental tasks.

TABLE II
OFFLINE TRAINING RESULTS

		A	B	C	D	E
	Trials	140	160	120	200	200
Accuracy (%)	Left-hand	79.0	88.8	96.6	86.0	78.5
	Right-hand	85.9	89.4	82.0	62.3	74.0
	Foot	59.3	75.3	83.2	63.8	75.0
	Average	74.7	84.5	87.3	70.7	75.8
ITR (bit/min)		7.7	12.1	13.6	6.4	8.2

TABLE III
ONLINE FEEDBACK TESTING RESULTS

		A	B	C	D	E
Response Time (sec)	T1	2.2	1.6	1.4	1.9	2.1
	T2	3.4	3.1	2.6	3.5	3.3
Accuracy (%)	Left-hand	86.7	80.0	100.0	93.3	86.7
	Right-hand	80.0	86.7	93.3	66.7	66.7
	Foot	66.7	73.3	86.7	66.7	73.3
	Average	77.8	80.0	93.3	77.8	75.6
ITR (bit/min)		10.6	12.8	26.5	10.4	9.8

Results(Navigation Performance)

- The results of the real-time navigation experiments of the humanoid robot.

- During the manual control experiments, all of the subjects controlled the robot to pass through all five waypoints without any collisions during navigation.

- During the BCI control experiments, the robot stepped on 3.2 waypoints with an average of 0.3 collisions, while the robot always successfully reached the final position.

Subject	Session	Total time (sec)	Distance travelled (cm)	Forward steps (times)	Turning steps (times)	Explored angle (°)	# Trans. (times)	Waypoint (times)	Collisions (times)
A	BCI	634.1	335.5	102.7	64.3	1161.3	39.7	2.3	0.7
	Manual	479.7	415.8	126.0	64.0	543.0	27.0	5.0	0.0
B	BCI	642.4	429.0	129.3	78.3	1485.9	40	4	0.7
	Manual	432.7	403.7	129.0	58.0	501	21	5	0
C	BCI	632.3	430.1	130.3	69.7	974.0	49.7	4.7	0.0
	Manual	452.9	389.4	118.0	64.0	605.0	34.0	5.0	0.0
D	BCI	448.8	307.0	86.7	46.0	704.9	31.3	2.0	0.0
	Manual	410.5	481.0	134.0	61.0	494.1	21.0	5.0	0.0
E	BCI	448.8	410.0	115.0	51.7	585.1	27.0	2.7	0.3
	Manual	424.4	508.9	143.0	58.0	509.0	24.0	5.0	0.0
BCI	Mean (± Std)	561.3 (± 102.8)	382.3 (± 57.2)	112.8 (± 18.5)	62.0 (± 13.2)	982.2 (± 360.7)	37.5 (± 8.8)	3.1 (± 1.2)	0.3 (± 0.4)
Manual	Mean (± Std)	440.0 (± 27.0)	439.8 (± 52.2)	130.0 (± 9.3)	61.0 (± 3.0)	530.4 (± 45.7)	25.4 (± 5.4)	5.0 (± 0.0)	0.0 (± 0.0)

Results(Navigation Performance)

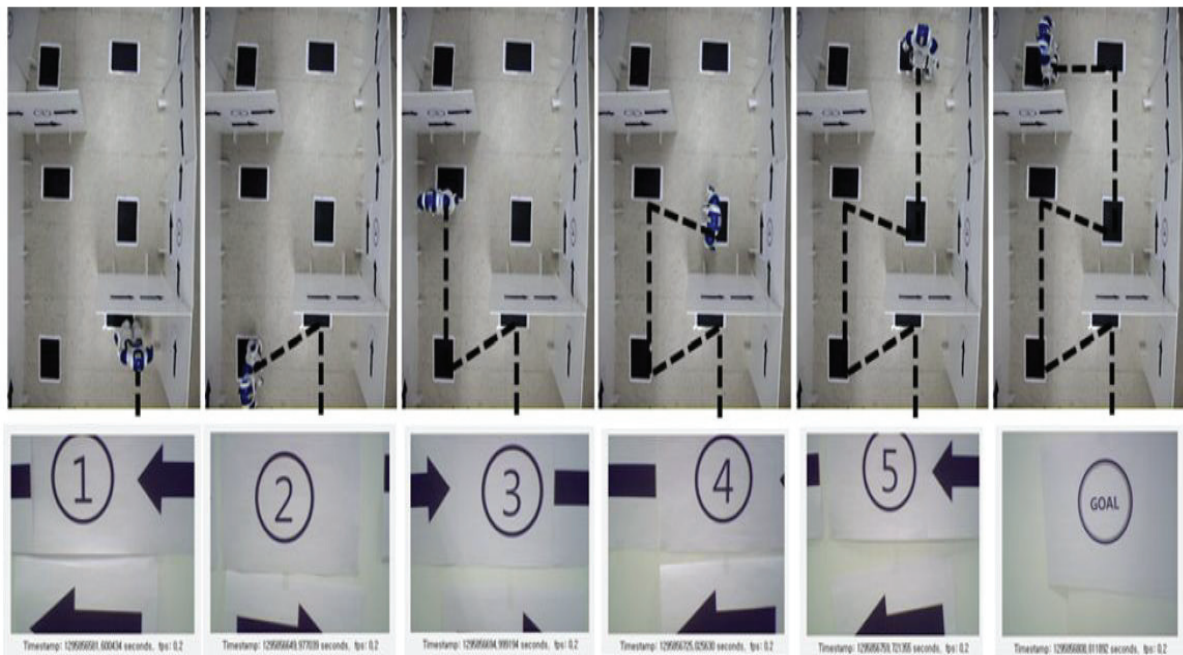- Fig. shows the sequential snapshots taken during an experiment.

Fig. 12. Navigation task is to make the robot move from a starting position to destination regions, while passing through the five waypoints at the corners of the maze. The first row shows snapshots taken during a trial, and the second row shows images acquired from the robot camera at each position.

Discussions

- This paper has described a new humanoid navigation system that is directly controlled through an asynchronous sensorimotor rhythm-based BCI system.

- Their approach allows for flexible robotic motion control in unknown environments using a camera vision.

- Brain-actuated humanoid control by this active BCI could be further improved in speed and accuracy.

- Recently, researchers have introduced hybrid BCIs that exploit the advantages of different reactive approaches (e.g., P300 or steady-state visually evoked potentials) and active approaches to improve the overall performance of BCI system.

- Another extension of this study is to realize human–robot interaction that can recognize high-level human cognitions, such as affective states.

Thank you!